

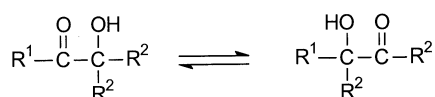
Asymmetric Catalysis, 132<sup>[†]</sup>Metal-Catalyzed Enantioselective  $\alpha$ -Ketol RearrangementsHenri Brunner<sup>\*[a]</sup> and Frank Stöhr<sup>[a]</sup>*Dedicated to Professor Heinrich Vahrenkamp on the occasion of his 60th birthday***Keywords:** Rearrangements / Isomerizations / Ketones / Asymmetric catalysis

Promoted by catalytic amounts of transition-metal complexes, the tertiary  $\alpha$ -hydroxy ketones **1**, **3**, **5/6** undergo  $\alpha$ -ketol rearrangements to afford equilibrium mixtures of isomers with a reorganization of the carbon skeleton. The range of metal complexes catalyzing the isomerizations is large; the best results were obtained with the catalyst systems NiCl<sub>2</sub>/TMEDA, Ni(acac)<sub>2</sub>, and Ni(acac)<sub>2</sub>/TMEDA (TMEDA = *N,N,N',N'*-tetramethyl-1,2-diaminoethane). The catalytic rearrangements were performed at 130 °C in the absence of solvent, with a Ni<sup>II</sup>/ligand/substrate ratio of 1:2:100. The equilibrium composition of the model system **1/2** is 12.5:87:5.

The conversion of the achiral substrates **1** and **3** into the chiral products **2** and **4** can be used for kinetic resolution. However, the reverse reactions **2**  $\rightarrow$  **1** and **4**  $\rightarrow$  **3** in the equilibrations narrow the window for asymmetric induction with enantioselective catalysts of the metal component/optically active ligand type. In system **1**, the highest enantiomeric excess was achieved with the catalyst systems NiCl<sub>2</sub>/pybox [18.9% (*S*)-**2**] and Ni(acac)<sub>2</sub>/pybox [19.3% (*R*)-**2**] {pybox = 2,6-bis[(*S*)-4-isopropyl(oxazolin-2'-yl)]pyridine}. The  $\alpha$ -ketol rearrangement of **3** with the Ni(acac)<sub>2</sub>/pybox catalyst resulted in a maximum enantiomeric excess of 37.1% (*S*)-**4**.

## Introduction

In the  $\alpha$ -ketol rearrangement of  $\alpha$ -hydroxy ketones of the type shown in Scheme 1, the carbonyl and hydroxy parts of the hydroxycarbonyl moiety change their roles. In the first step of the rearrangement, one of the substituents R<sup>2</sup> migrates from the hydroxy carbon atom to the carbonyl carbon atom. A proton shift completes the inversion of the carbonyl and hydroxy functionalities. In a subsequent step, the substituent R<sup>1</sup> may also take part in the rearrangement.

Scheme 1.  $\alpha$ -Ketol rearrangement

Isomerizations of  $\alpha$ -hydroxycarbonyl compounds are of crucial importance in metabolism. In vivo, these rearrangements are catalyzed by enzymes with high regio- and stereoselectivity.<sup>[1,2,3]</sup> In vitro, de Bruyn and van Ekenstein observed the first  $\alpha$ -ketol rearrangement in the base-catalyzed isomerization of aldoses at the end of the 19th century.<sup>[4,5]</sup> The first step of this reaction was the formation of an enediol, because in D<sub>2</sub>O solution the C2-hydrogen atom was replaced by deuterium.<sup>[6,7]</sup> Favorski investigated the acid-

catalyzed rearrangements of secondary and tertiary  $\alpha$ -ketols in alcoholic solvents at 130 °C after the addition of concentrated sulfuric acid.<sup>[8,9]</sup>

Elphimoff–Felkin induced the isomerization of  $\alpha$ -ketols with aluminium *tert*-butoxide at 80 °C. Her main interest was the determination of the equilibrium composition of the isomers involved. She found that the  $\alpha$ -ketols with an alkyl-CO functionality were more stable than the  $\alpha$ -ketols with an aryl-CO functionality.<sup>[10,11,12]</sup> In the EI mass spectra of  $\alpha$ -hydroxy ketones, there are often fragments of products from  $\alpha$ -ketol rearrangements. First it was assumed that this rearrangement was induced by electron impact.<sup>[13]</sup> However, it was later shown that it was due to catalysis by hot metal/metal oxide surfaces in the mass spectrometer.<sup>[14,15]</sup> Stevens investigated thermal  $\alpha$ -ketol rearrangements of tertiary  $\alpha$ -hydroxy ketones in biphenyl at 252 °C.<sup>[16]</sup>

Bilik studied the interaction of aldoses and molybdates in weakly acidic solutions.<sup>[17]</sup> He found a C2-epimerization of D-glucose and D-mannose affording an equilibrium D-glucose/D-mannose of 2.5:1 irrespective of whether he started from D-glucose or from D-mannose. Evidence for a stereospecific 1,2-rearrangement and *against* an enediol mechanism was presented.

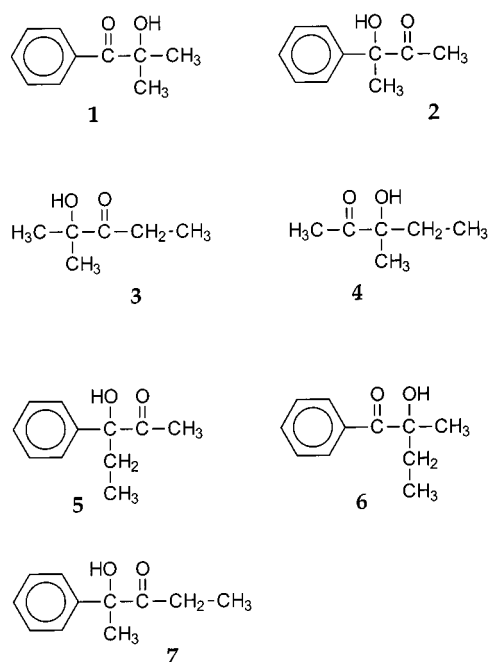
In 1983, Yoshikawa isolated a green complex from a solution containing a Ni<sup>II</sup>/TMEDA complex and D-mannose (TMEDA = *N,N,N',N'*-tetramethyl-1,2-diaminoethane).<sup>[18,19]</sup> Surprisingly, the same complex was isolated starting from D-glucose.<sup>[20]</sup> From these observations, Yoshikawa developed a C2-epimerization for aldoses under mild conditions (reaction time 3–4 min; temperature 60 °C;

<sup>[†]</sup> Part 131: H. Brunner, P. Schmidt, *Eur. J. Org. Chem.* **2000**, 2119–2133.

<sup>[a]</sup> Institut für Anorganische Chemie der Universität, D-93040 Regensburg, Germany  
Fax: (internat.) + 49-(0)941/943-4439  
E-Mail: henri.brunner@chemie.uni-regensburg.de

solvent MeOH; ratio  $\text{Ni}^{\text{II}}/\text{TMEDA}/\text{aldose} = 1:2:1$ ).<sup>[21,22,23]</sup> The mechanism of this reaction was examined with  $^{13}\text{C}$  aldoses. Starting from D-[1- $^{13}\text{C}$ ]glucose, only D-[1- $^{13}\text{C}$ ]glucose and D-[2- $^{13}\text{C}$ ]mannose were isolated after the standard epimerization procedure. The use of deuterated solvents for the reaction established the absence of a C–H bond cleavage. These results exclude an enediol mechanism and prove that a stereospecific C1/C2 exchange involving a rearrangement of the carbon skeleton takes place.<sup>[23]</sup>

We tried to extend the transition metal catalyzed  $\alpha$ -ketol rearrangement to tertiary  $\alpha$ -hydroxy ketones as simply as possible. In such  $\alpha$ -hydroxy ketones, the three additional substituents ( $\text{R}^1$  and  $\text{R}^2$  in Scheme 1) are methyl, ethyl, and phenyl (model systems **1/2**, **3/4**, and **5/6/7**, Scheme 2).



Scheme 2. Isomers of the model systems **1/2**, **3/4** and **5/6/7**

In the present paper we describe the synthesis and analysis of the components of the systems **1/2**, **3/4** and **5/6/7**, the preparative aspects of their transition metal catalyzed  $\alpha$ -ketol rearrangements and the stereochemical results of the  $\alpha$ -ketol rearrangements in **1/2** and **3/4** promoted by optically active transition metal catalysts.<sup>[24]</sup>

### The Model Systems **1/2**, **3/4**, and **5/6/7**

The achiral compound **1** is commercially available. In the isomerization of **1** the chiral isomer **2** is formed. The isomer analysis was carried out by  $^1\text{H}$  NMR spectroscopy and by gas chromatography on a Restek RT- $\beta$ DEX cst column, which allowed for the determination of the enantiomeric excess of **2**. The enantiomer analysis was also possible by  $^1\text{H}$  NMR spectroscopy using the shift reagent (*S*)-(+)-1-(9'-anthryl)-2,2,2-trifluoroethanol (super-Pirkle).

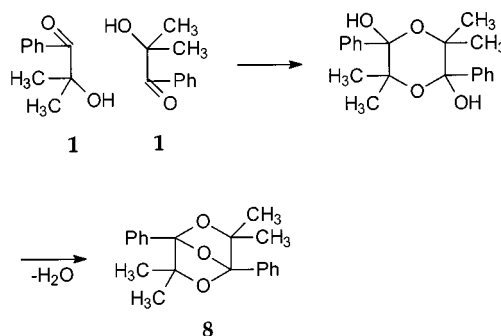
A 58:42 mixture of achiral **3** and racemic **4** was obtained by the Grignard reaction of 2,3-pentanedione with  $\text{MeMgCl}$ . The mixture was separated by fractional column

distillation to give pure **3**. The isomer and enantiomer analysis was performed analogously to model system **1/2**.

A 64:36 mixture of **5** and **6** was prepared by the reaction of 1-phenylpropane-1,2-dione with  $\text{EtMgCl}$ . The  $\alpha$ -ketol rearrangement of this mixture produced a third isomer **7**.  $^1\text{H}$  NMR spectroscopy was used for the isomer analysis.

### Isomerization of **1** – the $\text{NiCl}_2/\text{TMEDA}$ Catalyst

Using the reaction conditions of the epimerization D-glucose  $\rightleftharpoons$  D-mannose ( $\text{NiCl}_2/\text{TMEDA}/\text{aldose} = 1:2/1$ , solvent MeOH, temperature 65 °C) no isomerization of **1** was observed within 72 hours. Even a ratio of 1:10:20 did not result in any  $\alpha$ -ketol rearrangement of **1**. However, both starting material **1** and by-product **8** were found. The colorless crystalline **8** was formed in a base-catalyzed dimerization of **1** with subsequent dehydration (Scheme 3).



Scheme 3. Formation of **8**

In the following experiments, the reaction temperature was increased using higher boiling alcohols as solvents. With 1-butyl alcohol at 110 °C, the  $\alpha$ -ketol rearrangement of **1** was observed. However, besides **1** there were by-products derived from the solvent used. The unsuccessful search for better solvents led us to carry out the reaction in the absence of solvent. The mixture  $\text{NiCl}_2/\text{TMEDA}/\text{1} = 1:2:100$  is a yellow-green suspension at room temperature. On heating, the mixture becomes clear and a color change from green to red is observed at about 100 °C. The  $\alpha$ -ketol rearrangement of **1** starts at this temperature. Up to 110 °C the reaction is very slow, whereas above 140 °C the formation of by-products, especially **8**, increases. Therefore, 130 °C was chosen as the standard reaction temperature. The formation of by-products is negligible at this temperature.

Figure 1 shows how, starting from pure **1**, the concentration of **2** increases as a function of time for the reaction temperatures 110 °C and 130 °C at a ratio  $\text{NiCl}_2/\text{TMEDA}/\text{1} = 1:2:100$ .

The reaction is a first-order approach to an equilibrium  $\text{1} \rightleftharpoons \text{2}$  for which, according to many experiments,  $1/2 = 12.5:87.5$  is the best value. Given that in the isomerization of **1** at time  $t = 0$  there is no **2**, each measured point allows for the calculation of the rate constant  $k$  with the equation  $kt = \ln\{[2]_{\infty}/([2]_{\infty} - [2]_t)\}$  provided that the equilibrium concentration  $[2]_{\infty}$  is known. In this case, instead of the con-

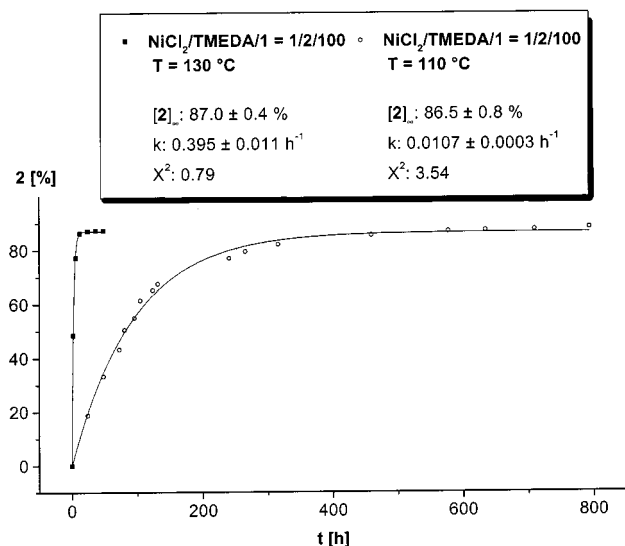


Figure 1.  $\text{NiCl}_2/\text{TMEDA}$ -catalyzed  $\alpha$ -ketol rearrangement of **1**: percentage of **2** as a function of time at the reaction temperatures 110 °C and 130 °C (no solvent)

centrations of **2**, it is possible to use the percentages of **2** directly. Deviations of the rate constant  $k$  from a constant value indicate the build-up or deactivation of different catalytically active species during the reaction. The curves in Figure 1 were fitted with the first-order formula and the calculated values for  $[2]_{\infty}$ ,  $k$  and  $X^2$  (sum of the squares of the deviations between the theoretical curve and the experimental points) are given with their errors in the inserts of Figure 1. At 110 °C the equilibrium is only reached after 600 hours. However, at 130 °C the equilibration is complete after 12 hours. In contrast to the epimerization of aldoses, which need equimolar quantities of catalyst, the  $\alpha$ -ketol rearrangement described here is a truly catalytic process.

Increasing the amount of substrate **1** ( $\text{NiCl}_2/\text{TMEDA}/\mathbf{1} = 1:2:1000$ ) reduces the isomerization rate appreciably. After 600 hours, only 70% of **2** is formed and the equilibrium is no longer reached. If the catalyst/substrate ratio is increased to 1:2:50, the reaction mixture takes a long time to become clear and at a ratio of 1:2:20 it remains a suspension. These higher catalyst concentrations increase the rates. However, the reproducibility of the results obtained with cloudy reaction mixtures is generally poor. Therefore, the ratio  $\text{NiCl}_2/\text{TMEDA}/\mathbf{1} = 1:2:100$  was chosen for the standard procedure. No  $\alpha$ -ketol rearrangement is induced by  $\text{NiCl}_2$  or by TMEDA alone, even at higher concentrations, proving that the isomerization is  $\text{Ni}^{\text{II}}/\text{TMEDA}$ -catalyzed.

In the epimerization D-glucose  $\rightleftharpoons$  D-mannose, a  $\text{NiCl}_2/\text{TMEDA}$  ratio of 1:2 has been used and the complex  $\text{Ni}_2(\text{TMEDA})_4\text{Cl}_2$  has been postulated as the catalytic species.<sup>[23]</sup> In order to prove that the same complex is active in the rearrangement of  $\alpha$ -hydroxy ketones, the isomerization of **1** was carried out with catalysts differing in the  $\text{NiCl}_2/\text{TMEDA}$  ratio (Figure 2). In these experiments, the percentage of **2** obtained after four hours of reaction time at 130 °C was determined. Up to a ratio  $\text{NiCl}_2/\text{TMEDA}$  1:1, there is hardly any isomerization of **1**. Obviously, the 1:1 complex  $[\text{Ni}(\text{TMEDA})]^{2+}$  is not a good catalyst for the  $\alpha$ -ketol re-

arrangement of **1**. With increasing TMEDA concentration, the 1:2 complex  $[\text{Ni}(\text{TMEDA})_2]^{2+}$  is formed and the percentage of **2** obtained after four hours rises appreciably. It remains constant up to a  $\text{NiCl}_2/\text{TMEDA}$  ratio of 1:8 (Figure 2). These observations provide evidence for a similar active species (and mechanism, see later) in the  $\text{NiCl}_2/\text{TMEDA}$ -catalyzed epimerization of aldoses and the isomerization of **1**.

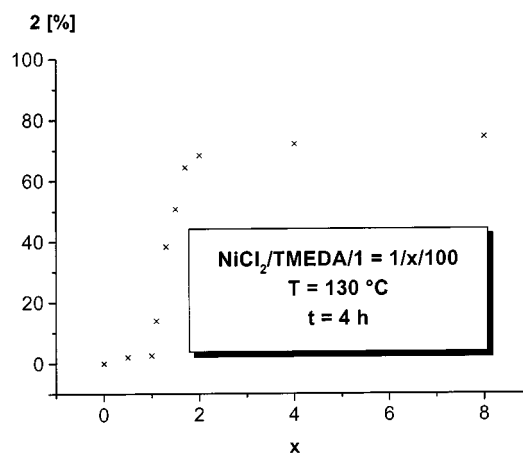


Figure 2.  $\text{NiCl}_2/\text{TMEDA}$ -catalyzed  $\alpha$ -ketol rearrangement of **1**: percentage of **2** after 4 hours reaction time at 130 °C as a function of the  $\text{NiCl}_2/\text{TMEDA}$  ratio  $1/x$

The water content of the  $\text{NiCl}_2$  used has no observable effect on the results of the catalyses. However, the reproducibility with anhydrous  $\text{NiCl}_2$  is better. Therefore, powdered anhydrous  $\text{NiCl}_2$  was used in the standard reactions.

## Isomerization of **1** – Other Catalysts

In the experiments to catalyze the  $\alpha$ -ketol rearrangement of **1** with other metal chlorides, the ligand TMEDA was used in a ratio  $M^{n+}/(\text{TMEDA})_n$ . With NaCl and KCl, as well as with  $\text{MgCl}_2$  and  $\text{CaCl}_2$  together with TMEDA, no isomerization of **1** is found and with  $\text{AlCl}_3$ ,  $\text{CuCl}_2$ , and  $\text{ZnCl}_2$  only a maximum of about 5% of **2** is obtained.  $\text{PdCl}_2$ , the higher homologue of  $\text{NiCl}_2$ , does not catalyze the  $\alpha$ -ketol rearrangement in combination with TMEDA.  $\text{LaCl}_3$ ,  $\text{CrCl}_3$ ,  $\text{MnCl}_2$ ,  $\text{FeCl}_2$ , and  $\text{CoCl}_2$  together with TMEDA catalyze the isomerisation of **1**, but the reaction rates are lower and the amounts of by-products higher than with  $\text{NiCl}_2$ .  $\text{NiF}_2$  does not catalyze the reaction, whereas with  $\text{NiBr}_2$ ,  $\text{NiI}_2$ ,  $\text{Ni}^{\text{II}}$  tartrate, and  $\text{Ni}^{\text{II}}$  dimethylglyoximate in combination with TMEDA, the  $\alpha$ -ketol rearrangement is observed with low reaction rates, and the equilibrium value of 87.5% of **2** is not attained.

None of the metal compounds tested so far catalyze the  $\alpha$ -ketol rearrangement of **1** without the ligand TMEDA. Therefore, it was a surprise to find that  $\text{Ni}(\text{acac})_2$  catalyzes the rearrangement without the addition of TMEDA. The rate constant is lower ( $k = 0.13 \text{ h}^{-1}$ ) than with  $\text{NiCl}_2/$

TMEDA ( $k = 0.40 \text{ h}^{-1}$ ), but with both catalysts there is a color change at  $100^\circ\text{C}$ . On addition of TMEDA to  $\text{Ni}(\text{acac})_2$  [ $\text{Ni}(\text{acac})_2/\text{TMEDA}/\mathbf{1} = 1:2:100$ ], the highest rate constant ( $k = 1.41 \text{ h}^{-1}$ ) so far was observed and the equilibration was complete within about 4 hours.  $\text{La}(\text{acac})_3$ ,  $\text{VO}(\text{acac})_2$ ,  $\text{MoO}_2(\text{acac})_2$ ,  $\text{Co}(\text{acac})_2$ ,  $\text{Co}(\text{acac})_3$ , and  $\text{Cu}(\text{acac})_2$  also catalyze the  $\alpha$ -ketol rearrangement of  $\mathbf{1}$  without the addition of TMEDA, but the rates are lower and the amounts of by-products higher than with  $\text{Ni}(\text{acac})_2$ . With  $\text{Na}(\text{acac})$ , the rearrangement stops at an early stage. The complexity of the phenomena is demonstrated by the fact that the reaction rate is lowered by the addition of TMEDA to  $\text{Cu}(\text{acac})_2$ , whilst for other acetylacetonates, the rates increase with the addition of TMEDA.

In further experiments it was tested whether in the  $\text{NiCl}_2/\text{TMEDA}$  catalyst the ligand TMEDA can be replaced by other ligands. With 1,4-diazabicyclo[2.2.2]octane (triethylenediamine) in a ratio  $\text{NiCl}_2/\text{triethylenediamine}/\mathbf{1} = 1:2:100$  and at a temperature of  $130^\circ\text{C}$ , the equilibrium is reached only after about 200 hours ( $k = 0.016 \text{ h}^{-1}$ ) and the color change from green to red is not reversible. The lower reaction rate relative to the TMEDA system ( $k = 0.40 \text{ h}^{-1}$ ) might be due to the higher rigidity of the triethylenediamine ligand. (*R,R*)-1,2-Diamino-1,2-diphenylethane together with  $\text{NiCl}_2$  ( $\text{NiCl}_2/\text{ligand}/\mathbf{1} = 1:2:50$ ) at  $130^\circ\text{C}$  gives a soluble blue-green complex, however, no isomerization is observed. Although the reaction mixtures with the ligand tri-*n*-butylamine at ratios of  $\text{NiCl}_2/\text{N}(\text{nBu})_3/\mathbf{1}$  from 1:1:100 to 1:2:100 at  $130^\circ\text{C}$  are cloudy, isomerization is found, in agreement with results that metal/monoamine complexes catalyze the epimerization of aldoses.<sup>[25]</sup>

The reaction rates are low and equilibrium is not reached with ratios  $\text{NiCl}_2/\text{N}(\text{nBu})_3/\mathbf{1}$  from 1:1:100 to 1:20:100. The  $\text{NiCl}_2/\text{N}(\text{nBu})_3/\mathbf{1}$  system exhibits a somewhat different concentration-dependence from the  $\text{NiCl}_2/\text{TMEDA}/\mathbf{1}$  system

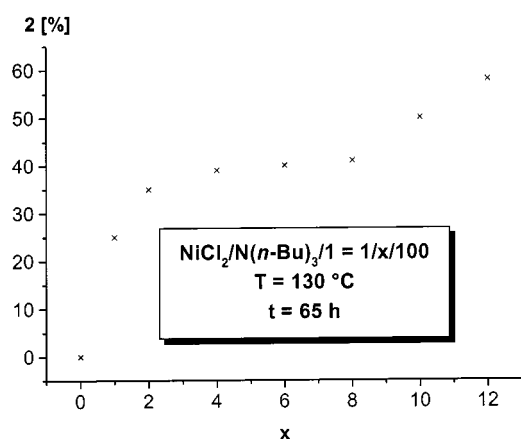


Figure 3.  $\text{NiCl}_2/\text{N}(\text{nBu})_3$ -catalyzed  $\alpha$ -ketol rearrangement of  $\mathbf{1}$ : percentage of  $\mathbf{2}$  after 65 hours reaction time at  $130^\circ\text{C}$  as a function of the  $\text{NiCl}_2/\text{N}(\text{nBu})_3$  ratio  $1/x$

(Figure 2). Figure 3 shows the percentage of  $\mathbf{2}$  obtained after 65 hours reaction time at  $130^\circ\text{C}$  as a function of the ratio  $\text{NiCl}_2/\text{N}(\text{nBu})_3/\mathbf{1}$ . While the system  $\text{NiCl}_2/\text{TMEDA}/\mathbf{1}$  reaches maximum activity at a ratio of 1:2:100, for the system  $\text{NiCl}_2/\text{N}(\text{nBu})_3/\mathbf{1}$ , the maximum activity is obtained at

a ratio of 1:4:100, indicating similar active species with one TMEDA ligand equivalent to two  $\text{N}(\text{nBu})_3$  ligands. Different from the TMEDA system, the percentage of  $\mathbf{2}$  increases in the  $\text{N}(\text{nBu})_3$  system at higher tri-*n*-butylamine concentrations.

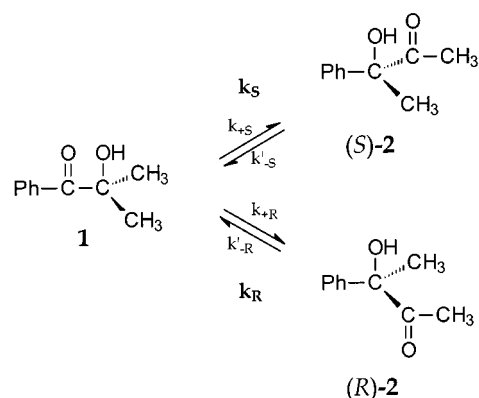
$\text{Ti}(\text{O}i\text{Pr})_4$  catalyzes the isomerization of  $\mathbf{1}$  without the addition of ligands. At a ratio  $\text{Ti}(\text{O}i\text{Pr})_4/\mathbf{1} = 1:100$ , a rate constant ( $k = 0.36 \text{ h}^{-1}$ ) comparable with the system  $\text{NiCl}_2/\text{TMEDA}$  ( $k = 0.40 \text{ h}^{-1}$ ) is found, in agreement with Elphimoff's investigations.<sup>[11]</sup> However,  $\text{NaOEt}$  does not catalyze the  $\alpha$ -ketol rearrangement of  $\mathbf{1}$ . Neither triphenylphosphane nor  $\text{NiCl}_2/\text{P}(\text{C}_6\text{H}_5)_3$  nor  $[\text{NiCl}_2(-)\text{-diop}]$  catalyze the equilibration  $\mathbf{1} \rightleftharpoons \mathbf{2}$ .  $[\text{NiCl}_2(\text{bpy})]$  catalyzes the isomerization at a low rate, but equilibrium is not reached. Pyridine and its combination with  $\text{NiCl}_2$  do not catalyze the reaction. With  $\text{NaOH}$ , at a  $\text{NaOH}/\mathbf{1}$  ratio = 1:100 no isomerization is observed and at a 1:10 ratio, decomposition occurs.

### Isomerization of $\mathbf{5/6}$ – Preliminary Experiments

The model system  $\mathbf{5/6/7}$  consists of three isomers. In the isomerization of a sample  $\mathbf{5/6} = 64.3:35.7$  with  $\text{NiCl}_2/\text{TMEDA}/\mathbf{5/6} = 0.5:1:20$  at a reaction temperature of  $130^\circ\text{C}$ , the third isomer  $\mathbf{7}$  is found and an isomer mixture  $\mathbf{5/6/7} = 52.9:17.4:29.7$  is obtained after 17 hours.

### Optical Induction – Theory

In the isomerization of prochiral  $\mathbf{1}$  to chiral  $\mathbf{2}$ , an asymmetric induction should be obtained provided that the rate constants  $k_S$  and  $k_R$  have different values (Scheme 4).



Scheme 4. Formation of the enantiomers (*S*)- and (*R*)- $\mathbf{2}$  in the  $\alpha$ -ketol rearrangement of  $\mathbf{1}$

In the initial phase of the equilibration  $\mathbf{1} \rightleftharpoons \mathbf{2}$ , one enantiomer may be formed faster than the other, depending on the ratio  $k_S/k_R = s$ . With increasing conversion, the enantiomeric excess will decrease and at equilibrium both enantiomers will have the same concentration. Figure 4 shows the theoretical curves for the (*S*)- $\mathbf{2}$ , (*R*)- $\mathbf{2}$ , and (*R/S*)- $\mathbf{2}$  concentrations as well as the enantiomeric excess. A first-order approach to an equilibrium of 87.5% of  $\mathbf{2}$  and 12.5% of  $\mathbf{1}$ , as found in the preparative studies, was assumed. The rate constants were arbitrarily adjusted to  $k_R = 1 \text{ h}^{-1}$  and  $k_S = 2 \text{ h}^{-1}$ . At complete conversion, a mixture of 87.5% of *ra*-



cemic **2** and 12.5% of **1** is obtained. Thus, the reaction must be stopped before complete conversion in order to find a compromise between yield and enantiomeric excess. In contrast to kinetic resolution, in which the chiral products do not revert to the starting material, in the equilibration  $\mathbf{1} \rightleftharpoons \mathbf{2}$  the reverse reaction will narrow the window for optical induction.

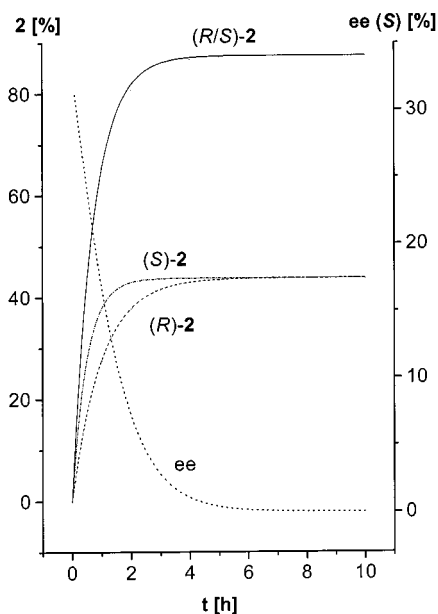


Figure 4. Theoretical curves for the equilibration  $\mathbf{1} \rightleftharpoons \mathbf{2}$  (87.5% of **2** and 12.5% of **1**) adjusted for  $k_R = 1 \text{ h}^{-1}$  and  $k_S = 2 \text{ h}^{-1}$  ( $s = 2$ )

### Optically Active Amines, Acetylacetonates, and Cinchona Alkaloids

The good preparative results obtained with the ligand TMEDA in combination with  $\text{NiCl}_2$  or  $\text{Ni}(\text{acac})_2$  suggested the use of optically active diamines as chiral ligands in the  $\alpha$ -ketol rearrangement of **1**. With (*S,S*)- and (*R,R*)-*N,N,N',N'*-tetramethyl-1,2-diamino-1,2-diphenylethane in combination with  $\text{NiCl}_2$  or  $\text{Ni}(\text{acac})_2$  there is a color change from green to red at  $100^\circ\text{C}$  and isomerization takes place, although with low rates ( $\text{NiCl}_2/\text{ligand}/\mathbf{1} = 1:2:100$ ;  $k = 0.09 \text{ h}^{-1}$  and  $\text{Ni}(\text{acac})_2/\text{ligand}/\mathbf{1} = 1:2:100$ ;  $k = 0.21 \text{ h}^{-1}$ ). However, no enantiomeric excess is observed. The primary diamine (*R,R*)-1,2-diamino-1,2-diphenylethane with  $\text{NiCl}_2$  does not catalyze the reaction. The systems  $\text{NiCl}_2$  or  $\text{Ni}(\text{acac})_2$  in combination with (*R*)-1-phenylethylamine in a ratio 0.5:1:100 are cloudy. With  $\text{Ni}(\text{acac})_2$  the equilibrium is reached, however, the enantiomeric excess is below 1%. With  $\text{NiCl}_2$ , the equilibration is slow and a maximum enantiomeric excess of 2.2% (*R*)-**2** is obtained.

Acetylacetonate was found to be a good ligand for the  $\alpha$ -ketol rearrangement of **1**, and the shift reagent  $\text{Eu}(\text{facam})_3$  (facam: 3-trifluoroacetyl-D-camphorate) was therefore tested. It catalyzes the isomerization of **2**, but no asymmetric induction is obtained.

With the alkaloid (+)-cinchonine in combination with  $\text{Ni}(\text{acac})_2$ , a color change takes place on heating, although less pronounced than with other  $\text{Ni}^{\text{II}}$ /ligand systems. With

a ratio  $\text{Ni}(\text{acac})_2/(+)\text{-cinchonine}/\mathbf{1} = 0.5:1:100$  at  $130^\circ\text{C}$ , the equilibrium  $\mathbf{1}/\mathbf{2} = 12.5:87.5 = \mathbf{1}/(\text{S})\text{-}\mathbf{2}/(\text{R})\text{-}\mathbf{2} = 12.5:43.75:43.75$  is reached with a rate constant  $k = 0.040 \text{ h}^{-1}$  within about 100 hours.

The build up of the (*S*)-**2** and (*R*)-**2** percentages as a function of the reaction time  $t$  is displayed in Figure 5. There was an excess of (*S*)-**2** during the reaction. Fitting of the curves yields the rate constants for the formation of the enantiomers  $k_S = 0.042 \text{ h}^{-1}$  and  $k_R = 0.038 \text{ h}^{-1}$  resulting in a stereoselectivity factor of  $s = k_S/k_R = 1.11$ .<sup>[26]</sup> The enantiomeric excess should decrease from a maximum at the start of the reaction. However, it increases first from 0 to 4% and drops thereafter (Figure 6). Furthermore, whereas the curve calculated from the rate constants  $k_S$  and  $k_R$  after 54 hours reaction time, when the ratio  $k_S/k_R = s$  reached a maximum, fits the experimental points at higher reaction times (Figure 6, dotted line), the curve calculated from the average rate constants  $k_S$  and  $k_R$  derived from Figure 5 deviates appreciably from the measured enantiomeric excess (Figure 6, bold line).

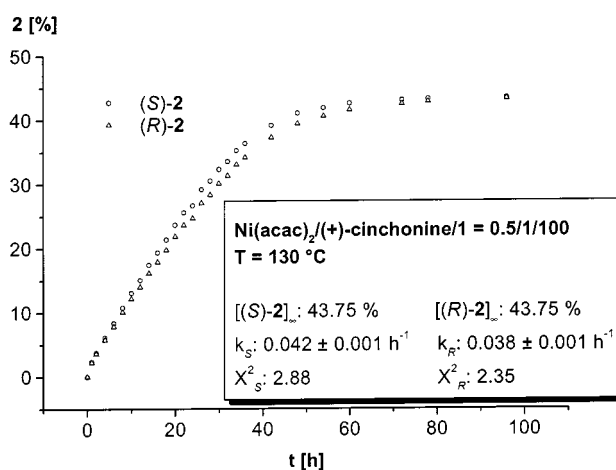


Figure 5. Percentage of (*S*)- and (*R*)-**2** as a function of reaction time

This behavior will be understood better after inspection of the curve of the rate constants (Figure 6, squares). Ideally, the rate constant  $k$  should be constant during a reaction. However, Figure 6 shows that this is not true for the  $\alpha$ -ketol rearrangement of **1** promoted by the catalyst  $\text{Ni}(\text{acac})_2/(+)\text{-cinchonine}$ . At the beginning of the reaction there are high rate constants which decrease after very short time. This could be due to  $\text{Ni}(\text{acac})_2$  which has been shown to be a good catalyst. Then, a new catalytically active species is building up. It may be the product of the reaction of  $\text{Ni}(\text{acac})_2$  with (+)-cinchonine, associated with the color change on heating. Parallel to this rate increase, the stereoselectivity factor rises to  $s = 1.20$ . After 70 hours, the rate constants decrease, probably owing to a successive deactivation of the catalytically active species.

(-)-Cinchonidine, the diastereomer of (+)-cinchonine, behaves analogously, but gives an excess of (*R*)-**2**. The average rate constant is  $k = 0.041 \text{ h}^{-1}$  [with (+)-cinchonine

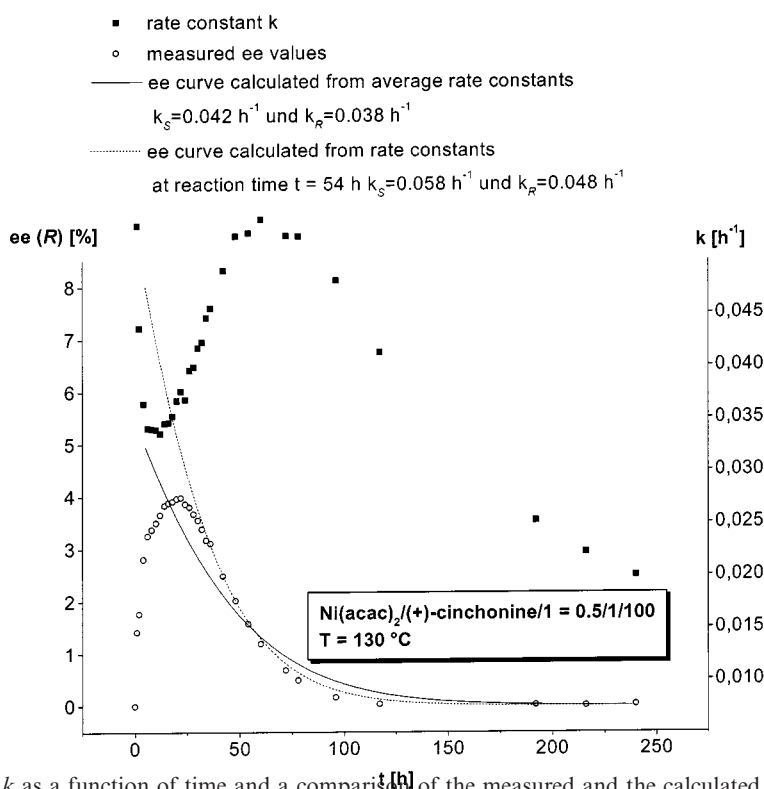


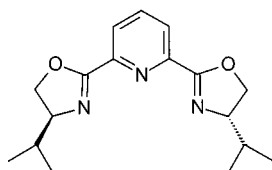
Figure 6. The rate constant  $k$  as a function of time and a comparison of the measured and the calculated enantiomeric excesses

$0.040 \text{ h}^{-1}$ ], the maximum enantiomeric excess is 5.5% (*R*)-**2** [4.0% (*S*)-**2**], the average stereoselectivity factor was  $s = 1.18$  ( $s = 1.11$ ) and the maximum stereoselectivity factor was  $s_{\text{max}} = 1.40$  ( $s_{\text{max}} = 1.20$ ). The system  $\text{NiCl}_2$ /(+)-cinchonine/**1** = 0.5:1:100 at  $130^\circ\text{C}$  is cloudy. The reproducibility of the catalyses is unsatisfactory and the enantiomeric excess is low.

The system  $\text{NiCl}_2$ /(+)-quinidine/**1** = 0.5:1:100 at  $130^\circ\text{C}$  is catalytically active with a rate constant  $k = 7.7 \times 10^{-3} \text{ h}^{-1}$  and a maximum enantiomeric excess of 1.4% (*S*)-**2**. In the system  $\text{Ni}(\text{acac})_2$ /(-)-*N*-methylephedrine/**1** = 1:1:100, the maximum enantiomeric excess was 4.6% (*R*)-**2** and the maximum stereoselectivity factor  $s = 1.23$ . (-)-Nicotine and (-)-strychnine in combination with  $\text{NiCl}_2$  give slow catalysis. The equilibrium is not reached and the enantioselectivity is small.<sup>[24]</sup>

### Optically Active Pyridineoxazolines

The best enantiomeric excess in the  $\alpha$ -ketol rearrangement of **1** is obtained with  $\text{Ni}^{\text{II}}$  complexes of the pyridine-oxazoline 2,6-bis[(*S*)-4-isopropyl(oxazolin-2'-yl)]pyridine<sup>[27]</sup> (pybox, Scheme 5).



Scheme 5. Ligand 2,6-bis[(*S*)-4-isopropyl(oxazolin-2'-yl)]pyridine (pybox)

At a ratio  $\text{NiCl}_2$ /pybox/**1** of 0.5:1:100 a soluble complex is formed, which shows a color change at  $100^\circ\text{C}$ . Figure 7 displays the percentage of **2** and the enantiomeric excess as a function of time. The enantiomeric excess increases to 17.7% (*S*)-**2** after 6 hours. It rises further to 18.3% after 24 hours and is still 17.9% after 72 hours. At this point the percentage of **2** had increased to 55% and the isomerization had almost come to a stop, as is evident from Figure 8, which shows the decrease of catalytic activity with time. Although conversion had almost ceased after 72 hours, the stereoselectivity had reached a maximum with  $s = 1.71$ .

Table 1 (entries 1–3) shows that increasing the catalyst concentration increases the percentage of **2**, although the equilibrium of 87.5% of **2** was not attained. The maximum enantioselective excesses hardly differ, whereas the maximum stereoselectivity factors rise with the catalyst concentration. Increasing the Ni content in the  $\text{NiCl}_2$ /pybox catalyst from 1:4, to 1:2 to 1:1.33 (Table 1, entries 4–6) does not change the kinetic and stereochemical parameters. However, ratios of  $\text{NiCl}_2$ /pybox = 1:1 and greater decrease the values for **2**,  $ee_{\text{max}}$ , and  $s_{\text{max}}$  dramatically (Table 1, entries 7, 8), indicating that the  $\text{Ni}^{\text{II}}$ /pybox complex of stoichiometry 1:1 is not a good catalyst for the  $\alpha$ -ketol rearrangement.

$\text{NiF}_2$ ,  $\text{NiBr}_2$ ,  $\text{NiI}_2$ , and  $\text{Ni}(\text{dmg})_2$  (dmg = dimethylglyoximate) do not rival  $\text{NiCl}_2$  in the system  $\text{NiX}_2$ /pybox/**1** = 0.5:1:100 in rate and enantioselectivity. Surprisingly,  $\text{Ni}(\text{acac})_2$  turns out to be the best Ni component by far in the system  $\text{NiX}_2$ /pybox/**1**. At a ratio  $\text{Ni}(\text{acac})_2$ /pybox/**1** = 0.5:1:100 at  $130^\circ\text{C}$  there is an equilibration of 87.5% of **2**  $\rightleftharpoons$  12.5% of **1** after 36 hours. Whilst all the other nickel com-

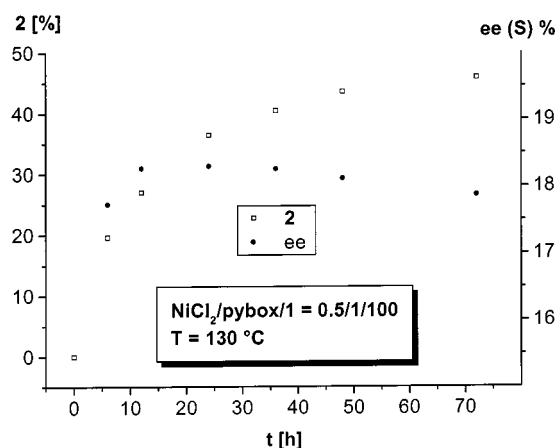


Figure 7. Percentage of **2** and enantiomeric excess as a function of time

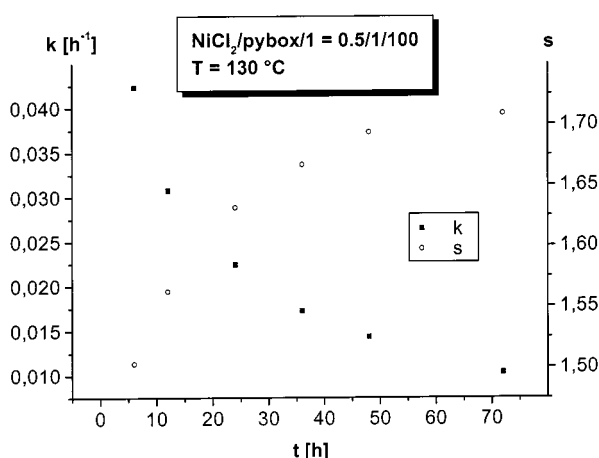


Figure 8. Stereoselectivity factor *s* and rate constant *k* as a function of time

pounds tested give an excess of (*S*)-**2**, with Ni(acac)<sub>2</sub> an enantiomeric excess of (*R*)-**2** is obtained. Figure 9 displays the percentage and enantiomeric excess of **2** as a function of time.

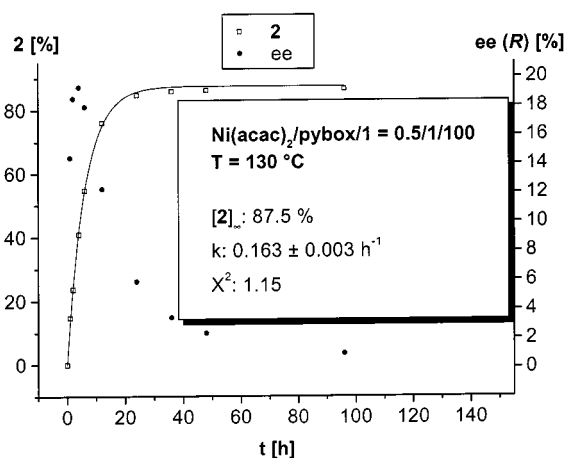


Figure 9. Percentage of **2** and enantiomeric excess as a function of time

The enantiomeric excess rises at the beginning of the reaction because the enantioselective catalyst has to be formed first. The enantiomeric excess reaches a maximum of 19.3% of (*R*)-**2** after four hours, then it decreases rapidly. After 96 hours, only an enantiomeric excess of 0.9% is observable. In this reaction too, many catalytically active species must be involved, because the stereoselectivity factor adopts a manifold of values passing through a maximum of *s* = 3.46.

In addition to the 2,6-pyridinebisoxazoline pybox, another twelve oxazoline derivatives (bisoxazolines, 2-salicyl- and 2-pyridineoxazolines) were tested in combination with NiCl<sub>2</sub> or Ni(acac)<sub>2</sub> in the  $\alpha$ -ketol rearrangement of **1**. None of these ligands reached activities and enantioselectivities as high as the pybox ligand.<sup>[24]</sup>

While pybox in combination with NiCl<sub>2</sub> catalyzes the  $\alpha$ -ketol rearrangement of **1**, no rearrangement of **3** is found with an NiCl<sub>2</sub>/pybox/**3** ratio = 0.5:1:100, even though a soluble complex is formed which shows a color change at 100 °C. However, the system Ni(acac)<sub>2</sub>/pybox/**3** = 0.5:1:100 catalyzes the isomerization of **3** at a reaction temperature of 130 °C. Figure 10 displays the concentration of **4** and the enantiomeric excess as a function of time.

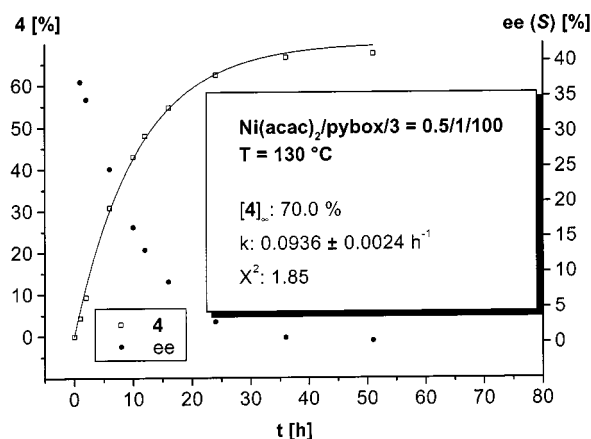


Figure 10. Percentage of **4** and enantiomeric excess as a function of time

The reaction is a first-order approach to an equilibrium of 70.0% of **4** and 30% of **3**. This equilibrium composition was confirmed by catalyses with NiCl<sub>2</sub>/TMEDA starting from pure **3** and from a 8% of **3**:92% of **4** mixture. The enantiomeric excess decreases from 37.1% (*S*)-**4** (Figure 10) as does the stereoselectivity factor from *s* = 2.23.

Increasing the catalyst concentration from 0.5:1:250 to 0.5:1:100 increases the rate constants, the maximum enantiomeric excess and the maximum stereoselectivity factor. Another increase to 0.5:1:25 leads to a higher reaction rate, but *ee*<sub>max</sub> and *s*<sub>max</sub> decrease (Table 2, entries 1–3). Increasing the ratio Ni(acac)<sub>2</sub>/pybox from 0.25:1 to 0.5:1 increases the reaction rate, the maximum enantiomeric excess and the maximum stereoselectivity factor. Higher Ni(acac)<sub>2</sub> concentrations, however, lead to a decrease of the rate and the equilibrium is no longer reached (Table 2, entries 4–6).

Table 1. Effect of the catalyst concentration and the NiCl<sub>2</sub>/pybox ratio on the catalysis of the isomerization **1** ⇌ **2**

Entry	NiCl <sub>2</sub> /pybox/ <b>1</b>	<b>2</b> [%] <sup>[a]</sup>	<i>t</i> [h]	<i>ee</i> <sub>max</sub> (S) [%] <sup>[a]</sup>	<i>t</i> [h]	<i>s</i> <sub>max</sub> <sup>[a]</sup>	<i>t</i> [h]
1	0.5:1:250	16.9	96	17.3	36	1.47	36
2	0.5:1:100	45.9	72	18.3	24	1.71	72
3	0.5:1:50	57.6	96	18.9	6	1.90	96
4	0.25:1:100	45.1	72	18.6	12	1.75	72
5	0.5:1:100	45.9	72	18.3	24	1.71	72
6	0.75:1:100	44.4	50	18.3	12	1.69	50
7	1:1:100	11.2	50	14.0	6	1.35	6
8	2:1:100	6.11	50	1.68	6	1.03	6

<sup>[a]</sup> The values shown are the maximum values of a series of measurements.

Table 2. Effect of the catalyst concentration and the Ni(acac)<sub>3</sub>/pybox ratio on the catalysis of the isomerization **3** ⇌ **4**

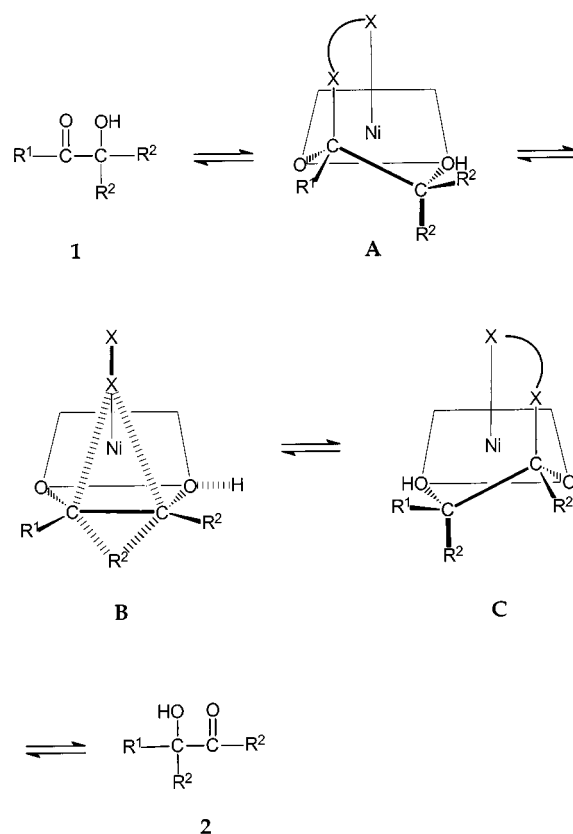
Entry	NiCl <sub>2</sub> /pybox/ <b>3</b>	<b>4</b> [%] <sup>[a]</sup>	<i>t</i> [h]	<i>ee</i> <sub>max</sub> (S) [%] <sup>[a]</sup>	<i>t</i> [h]	<i>s</i> <sub>max</sub> <sup>[a]</sup>	<i>t</i> [h]
1	0.5:1/250	22.9	36	14.8	6	1.36	6
2	0.5:1/100	67.2	51	37.1	1	2.23	1
3	0.5:1/25	70	36	34.5	1	2.19	1
4	0.25:1/100	28.0	26	16.3	12	1.46	12
5	0.5:1/100	67.2	51	37.1	1	2.23	1
6	1:1/100	54.2	39	34.9	3	2.19	3

<sup>[a]</sup> The values shown are the maximum values of a series of measurements.

## Mechanism

For the Ni<sup>II</sup>/TMEDA-catalyzed α-ketol equilibration **1** ⇌ **2**, we propose the mechanism shown in Scheme 6 as the first step. The substrate **1** coordinates to the Ni catalyst through the carbonyl oxygen and hydroxy oxygen atoms, forming a five-membered chelate ring. In **A**, one of the NMe<sub>2</sub> groups of the TMEDA ligand binds to Ni in a position facial to the O,O'-chelate of the substrate, whereas the other NMe<sub>2</sub> group adds to the carbonyl group of the chelate ligand converting the sp<sup>2</sup> carbon atom into the sp<sup>3</sup> carbon atom of a carbinolamine. In a kind of windshield wiper motion, the carbinolamine nitrogen atom passes over from the carbonyl carbon to the hydroxy carbon atom via transition state **B**. Simultaneously, the axial substituent R<sup>2</sup> on the other side of the chelate ligand migrates in the opposite direction. These processes are accompanied by a flip of the chelate ring to give **C**. A proton shift completes the role change of carbonyl and hydroxy parts. The carbinolamine-assisted rearrangement of the carbon skeleton in the substrate **1** is analogous to that proposed for the Ni<sup>II</sup>/TMEDA-catalyzed epimerization glucose ⇌ mannose.<sup>[23]</sup>

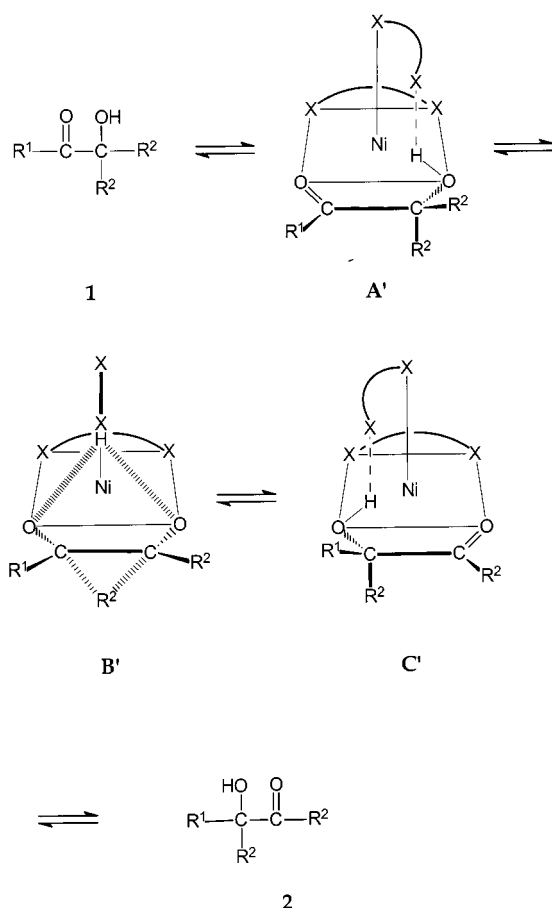
The simplified mechanism in Scheme 6 does not account for the fact that the active isomerization catalysts have a stoichiometry Ni<sup>II</sup>/chelate = 1:2. Maybe one of the bidentate ligands must coordinate to Ni<sup>II</sup> as a normal chelate to allow the second ligand to bind as shown for X–X in Scheme 6 and to assist the rearrangement.

Scheme 6. Carbinolamine mechanism in the Ni(X–X)<sub>2</sub>-catalyzed rearrangement of α-ketols of the type **1** ⇌ **2** (charges disregarded)

Attack of the NMe<sub>2</sub> group of the TMEDA ligand on the carbonyl carbon atom generates a new chiral center, which can adopt an (*R*) or (*S*) configuration, depending on which of the two facial positions at Ni with respect to the O,O'-chelate is occupied. The stereochemical implication is that, of the two substituents at the hydroxy carbon (in Scheme 6 both are R<sup>2</sup>), only the axial one is able to take part in the stereospecific rearrangement. After dissociation and recoordination of **2**, the configuration at the carbinolamine carbon may invert and the substituent R<sup>1</sup> may participate in subsequent reaction steps. As long as the system is not at equilibrium, chiral inductions can be obtained by additional optically active ligands. Possibly, the surprising effect of the acetylacetonate ligand observed in the present study has the same origin as the TMEDA effect. An acetal-like structure with X–X = acetylacetonate in Scheme 6 could be formed assisting the rearrangement.

There is an alternative to the mechanism shown in Scheme 6. The dangling NMe<sub>2</sub> group of the unidentate X–X ligand can act as a base and bind to the proton of the OH group in **A'**, which has become relatively acidic on coordination. A move over to the other side via transition state **B'** could accompany the migration of R<sup>2</sup> from the hydroxy side to the carbonyl side (Scheme 7). Both mechanisms, the carbinolamine-assisted and the acid/base-assisted rearrangements, are interesting examples of bifunctional catalysis: Ni<sup>II</sup> catalysis through coordination and nucleophilic assistance through the dangling end of a unidentate ligand.





Scheme 7. Acid-base assistance in the  $\text{Ni}(\text{X}-\text{X})_2$ -catalyzed rearrangement of  $\alpha$ -ketols of the type **1**  $\rightleftharpoons$  **2** (charges disregarded)

## Experimental Section

**General Remarks:** All reactions were performed under dried nitrogen. All reagents were of best commercial grade. Solids were used without further purification, liquids were dried with molecular sieves 4 Å for 24 h and distilled under nitrogen. —  $^1\text{H}$  and  $^{13}\text{C}$  NMR: Bruker AC 250 or ARX 400 (internal standard TMS). — Bulb-to-bulb distillations: Büchi GKR-50. — Kinetic calculations: Origin 5.0 by Microcal.

**2-Hydroxy-2-methyl-1-phenylpropane-1-one (1):** The commercial product was distilled under argon before use. The content of **2** in these samples varied by up to one percent as shown by GC analysis. For catalytic reactions, only samples with a content of **2** below 0.1% were used. Protected from light, compound **1** is stable for months. Isomerization of **1** gives a mixture of 3-hydroxy-3-phenylbutane-2-one (**2**) and **1** as a colorless liquid.

**1/2:** B.p. 60 °C/0.075 Torr. —  $^1\text{H}$  NMR (250 MHz,  $\text{CDCl}_3$ ):  $\delta$  = 1.62 [s, 6 H,  $\text{C}(\text{OH})(\text{CH}_3)_2$ , **1**], 1.77 [s, 3 H,  $\text{C}(\text{OH})\text{CH}_3$ , **2**], 2.08 (s, 3 H,  $\text{COCH}_3$ , **2**), 4.12 (sb, 1 H, OH, **1**), 4.57 (bs, 1 H, OH, **2**), 7.26–7.41 (m, 5 H,  $\text{CH}_{\text{arom}}$ , **2**), 7.43–7.61 (m, 3 H,  $\text{CH}_{\text{arom}}$ , **1**), 7.99–8.04 (m, 2 H,  $\text{CH}_{\text{arom}}$ , **1**). After addition of a threefold excess (by weight) of super-Pirkle to the NMR sample, the  $\text{C}(\text{OH})\text{CH}_3$  singlet of **2** splits, allowing for enantiomer analysis. The signal shifted upfield correlates with (+)-(R)-**2**.

**GC analysis of 1/2:** Hewlett Packard 5890A, split injector (250 °C), FID detector (260 °C), Spectra-Physics SP 4270 integrator, oven

temperature 110 °C, hydrogen as carrier gas, solvent  $\text{CH}_2\text{Cl}_2$ . Baseline separation was observed with a Restek Rt- $\beta$ DEX cst column (length 30 m, lumen 0.32 mm, film thickness 0.25  $\mu\text{m}$ ). Retention times: 19.0 min (–)-(S)-**2**, 19.6 min (+)-(R)-**2**, 25.4 min **1**. The assignment optical rotation/configuration is based on enantiomerically enriched samples.<sup>[17]</sup>

**2-Hydroxy-2-methylpentane-3-one (3) and 3-Hydroxy-3-methylpentane-2-one (4):** To an ice-cold solution of 2,3-pentanedione (78.2 mL, 75.1 g, 0.75 mol) in diethyl ether (750 mL) was added dropwise methylmagnesium chloride (250 mL, 0.75 mol, 3 mol/L) in THF (Merck) with stirring. When the addition was complete, the thick yellow mixture was allowed to warm up to room temperature and hydrolyzed by pouring it into an ice-cold saturated aqueous solution of ammonium chloride. The mixture was extracted with diethyl ether ( $4 \times 150$  mL). The combined organic layers were washed with water ( $3 \times 100$  mL), dried with  $\text{Na}_2\text{SO}_4$ , and the solvent was removed. The yellow liquid was distilled at 60–61 °C/25 Torr with a 50-cm Vigreux column to yield 55.5 g of a colorless liquid consisting of a 58:42 mixture of **3** and **4**. By very slow distillation with a Fischer 30-cm Spaltrohr column, it was possible to obtain pure **3** (colorless liquid) as the last fraction.

**3:** B.p. 61 °C/25 Torr. —  $\text{C}_6\text{H}_{12}\text{O}_2$  (116.16): calcd. C 62.04, H 10.41; found C 61.76, H 10.34. —  $^1\text{H}$  NMR (250 MHz,  $\text{CDCl}_3$ ):  $\delta$  = 1.09 (t,  $^3J$  = 7.3 Hz, 3 H,  $\text{CH}_2\text{CH}_3$ ), 1.36 (s, 6 H,  $\text{CH}_3$ ), 2.57 (q,  $^3J$  = 7.3 Hz, 2 H,  $\text{CH}_2$ ), 3.80 (sb, 1 H, OH).

Compound **4** was enriched to 92% by distillation with a Fischer 30-cm Spaltrohr column (colorless liquid) as the first fraction.

**4:** B.p. 61 °C/25 Torr. —  $\text{C}_6\text{H}_{12}\text{O}_2$  (116.16): calcd. C 62.04, H 10.41; found C 62.23, H 10.49. —  $^1\text{H}$  NMR (250 MHz,  $\text{CDCl}_3$ ):  $\delta$  = 0.80 (t,  $^3J$  = 7.4 Hz, 3 H,  $\text{CH}_2\text{CH}_3$ ), 1.34 [s, 3 H,  $\text{C}(\text{OH})\text{CH}_3$ ], 1.67–1.78 (m, 2 H,  $\text{CH}_2$ ), 2.19 (s, 3 H,  $\text{COCH}_3$ ), 3.80 (sb, 1 H, OH). — After addition of a fourfold excess (by weight) of super-Pirkle to the NMR sample, the signals of  $\text{C}(\text{OH})\text{CH}_3$  and  $\text{CH}_2\text{CH}_3$  split, enabling enantiomeric analysis. The upfield-shifted signal of  $\text{CH}_2\text{CH}_3$  and the downfield-shifted signal of  $\text{C}(\text{OH})\text{CH}_3$  correlate with (+)-(S)-**4**.

**GC Analysis of 3/4:** Hewlett Packard 9000, split injector (250 °C), FID detector (250 °C), Spectra-Physics SP 4290 integrator, oven temperature 88 °C, helium as carrier gas, solvent  $\text{CH}_2\text{Cl}_2$ . Baseline separation was observed with a Macherey–Nagel Lipodex-E column (length 50 m, lumen 0.25 mm). Retention times: 11.3 min **3**, 12.1 min (+)-(S)-**4**, 12.6 min (–)-(R)-**4**. The assignment optical rotation/configuration is based on enantiomerically enriched samples.<sup>[28]</sup>

**3-Hydroxy-3-phenylpentane-2-one (5) and 2-Hydroxy-2-methyl-1-phenylbutane-1-one (6):** Magnesium powder (4.86 g, 0.20 mol), flame-dried in a nitrogen-atmosphere, was suspended in diethyl ether (100 mL). 1-Bromoethane (15 mL, 21.79 g, 0.20 mol) in diethyl ether (100 mL) was added dropwise, keeping the mixture gently refluxing. After cooling to –40 °C, 1-phenylpropane-1,2-dione (24.8 g, 0.17 mol) was added dropwise with vigorous stirring. When the addition was complete, the mixture was worked up as described for **3/4**. Bulb-to-bulb distillation at 50–55 °C/2 Torr gave 13.1 g of a pale yellow liquid consisting of a 64:36 mixture of **5** and **6**.

**5/6:** B.p. 50–55 °C/2 Torr. —  $\text{C}_{11}\text{H}_{14}\text{O}_2$  (178.23): calcd. C 74.13, H 7.92; found C 74.56, H 7.85. —  $^1\text{H}$  NMR (250 MHz,  $\text{CDCl}_3$ ):  $\delta$  = 0.84 (t,  $^3J$  = 7.4 Hz, 3 H,  $\text{CH}_2\text{CH}_3$ , **6**), 0.93 (t,  $^3J$  = 7.4 Hz, 3 H,  $\text{CH}_2\text{CH}_3$ , **5**), 1.61 [s, 3 H,  $\text{C}(\text{OH})\text{CH}_3$ , **6**], 1.91–2.31 (m,  $2 \times 2$  H,

$\text{CH}_2$ , **5/6**), 2.08 (s, 3 H,  $\text{COCH}_3$ , **5**), 4.00–4.40 (sb, 1 H, OH, **6**), 4.40–4.65 (sb, 1 H, OH, **5**), 7.26–8.13 (m,  $2 \times 5$  H,  $\text{CH}_{\text{arom}}$ , **5/6**).

During isomerization 2-hydroxy-2-phenylpentane-3-one (**7**) is formed and a mixture of the three isomers **5/6/7** was obtained as a colorless liquid.

**7**:  $^1\text{H}$  NMR (250 MHz,  $\text{CDCl}_3$ ):  $\delta$  = 0.96 (t,  $^3J$  = 7.3 Hz, 3 H,  $\text{CH}_2\text{CH}_3$ ), 1.77 (s, 3 H,  $\text{C}(\text{OH})\text{CH}_3$ ), 2.30–2.54 (m, 2 H,  $\text{CH}_2$ ), 3.50–4.50 (sb, 1 H, OH), 7.26–8.13 (m, 5 H,  $\text{CH}_{\text{arom}}$ ).

**Standard Isomerization Procedure for the  $\alpha$ -Ketol Rearrangement of the Model Systems 1/2, 3/4, and 5/6/7:** All catalyses were performed under nitrogen in long Schlenk tubes with 10.0 mmol of substrate (1.52 mL **1**, 1.21 mL **3**, 1.78 g **5/6**). After the addition of the metal salt, the ligand, the substrate and a stirring bar, the Schlenk tube was kept at the required temperature. Aliquots (0.1 mL) were taken for analysis. The sample was dissolved in  $\text{CHCl}_3$  and filtered through a Pasteur pipette filled with silica (5 cm). After removal of the solvent, the sample was purified by bulb-to-bulb distillation and analyzed by  $^1\text{H}$  NMR spectroscopy and GC. Enlarged runs give identical results.

## Acknowledgments

We thank the Fonds der Chemischen Industrie for financial support and Prof. H. B. Kagan for helpful discussions.

- [1] F. B. Armstrong, E. L. Lipscomb, D. H. G. Crout, M. B. Mitchell, S. R. Prakash, *J. Chem. Soc., Perkin Trans. 1* **1983**, 1197–1201.
- [2] D. H. G. Crout, J. Littlechild, S. M. Morray, *J. Chem. Soc., Perkin Trans. 1* **1986**, 105–108.
- [3] D. H. G. Crout, D. L. Rathbone, *J. Chem. Soc., Chem. Commun.* **1988**, 98–99.
- [4] C. A. Lobry de Bruyn, W. Alberda van Ekenstein, *Recl. Trav. Chim. Pays-Bas* **1895**, 14, 195–216.
- [5] C. A. Lobry de Bruyn, W. Alberda van Ekenstein, *Recl. Trav. Chim. Pays-Bas* **1897**, 16, 256–261.
- [6] *Reaktionen der organischen Chemie* (Eds.: H. Krauch, W. Kunz), 5. Aufl., Dr. Alfred Hüthig Verlag, Heidelberg, **1976**, p. 760.
- [7] H. S. El Khadem, S. Ennifar, H. S. Isbell, *Carbohydr. Res.* **1989**, 185, 51–59.
- [8] N. A. Domin, *Zh. Obshch. Khim.* **1960**, 30, 705–716.
- [9] A. Favorski, *Bull. Soc. Chim. Fr.* **1926**, 216–220.
- [10] I. Elphimoff-Felkin, *Bull. Soc. Chim. Fr.* **1956**, 1845–1856.
- [11] I. Elphimoff-Felkin, P. Colard, M. Verrier, *Bull. Soc. Chim. Fr.* **1961**, 516–520.
- [12] I. Elphimoff-Felkin, *Bull. Soc. Chim. Fr.* **1967**, 1052–1057.
- [13] M. J. Frearson, D. M. Brown, *J. Chem. Soc. (C)* **1968**, 2909–2912.
- [14] C. Djerassi, *J. Chem. Soc. (C)* **1969**, 2550–2552.
- [15] R. T. Aplin, M. J. Frearson, *Chem. Ind. (London)* **1969**, 1663–1664.
- [16] C. L. Stevens, F. E. Glenn, P. M. Pillai, *J. Am. Chem. Soc.* **1973**, 95, 6301–6308.
- [17] V. Bilik, *Chem. Zvesti* **1972**, 26, 187–189.
- [18] H. Shioi, S. Yano, K. Toriumi, T. Ito, S. Yoshikawa, *J. Chem. Soc., Chem. Commun.* **1983**, 201–202.
- [19] T. Tanase, K. Kurihara, S. Yano, K. Kobayashi, T. Sakurai, S. Yoshikawa, *J. Chem. Soc., Chem. Commun.* **1985**, 1562–1563.
- [20] T. Tanase, F. Shimizu, S. Yano, S. Yoshikawa, *J. Chem. Soc., Chem. Commun.* **1986**, 1001–1003.
- [21] T. Tanase, F. Shimizu, M. Kuse, S. Yano, S. Yoshikawa, M. Hidai, *J. Chem. Soc., Chem. Commun.* **1987**, 659–661.
- [22] T. Tanase, F. Shimizu, M. Kuse, S. Yano, M. Hidai, S. Yoshikawa, *Inorg. Chem.* **1988**, 27, 4085–4094.
- [23] H. Brunner, D. Opitz, *J. Mol. Catal. A* **1997**, 118, 273–282.
- [24] F. Stöhr, Ph.D. thesis, Universität Regensburg, **1999**.
- [25] T. Tanase, T. Murata, S. Yano, M. Hidai, S. Yoshikawa, *Chem. Lett.* **1987**, 1409–1412.
- [26] H. B. Kagan, J. C. Fiaud, in: *Top. Stereochem.*, Vol. 18, (Eds.: E. L. Eliel, S. H. Wilen), J. Wiley & Sons Inc., New York, **1988**, p. 254.
- [27] H. Nishiyama, M. Kondo, T. Nakamura, K. Itoh, *Organometallics* **1991**, 10, 500–508.
- [28] D. H. G. Crout, C. R. McIntyre, N. W. Alcock, *J. Chem. Soc., Perkin Trans. 2* **1991**, 53–62.

Received January 12, 2000  
[O00013]